

Article

Decentralized Model-Reference Adaptive Control Based Algorithm for Power Systems Inter-Area Oscillation Damping

Tswa-wen Pierre-Patrick Banga-Banga ^{*}, Carl Kriger ^{*} and Yohan Darcy Mfoumboulou ^{*}

Centre for Substation Automation and Energy Management Systems (CSAEMS), Department of Electrical, Electronics and Computer Engineering, Cape Peninsula University of Technology, Cape Town 7500, South Africa

^{*} Correspondence: 211132500@mycput.ac.za (T.-w.P.-P.B.-B.); krigerc@cput.ac.za (C.K.); mfoumboulou@cput.ac.za (Y.D.M.)

Abstract: Being the primary cause of inter-area oscillations and due to the fact that they limit the generation's output, Low-Frequency Electromechanical Oscillations (LFEOs) represent a real threat to power system networks. Mitigating their effects is therefore crucial as it may lead to system collapse if not properly damped. As rotor angle instability is the primary cause of LFEOs, this paper presents a novel Model-Reference Adaptive Control (MRAC) scheme that enhances its stability. The proposed scheme is tested using the Single-Machine Infinite Bus (SMIB) network. The results obtained validate the proposed decentralized control architecture. The robustness of this oscillation damping controller is verified through simulations in MATLAB/SIMULINK. With Gaussian noise added to the structure of the generator to emulate small load variations responsible for the rotor angle instability, the results of the simulations show that the rotor angle remains stable. Furthermore, when subjected to faults, the recovery time is less than 500 ms.



Citation: Banga-Banga, T.-w.P.-P.; Kriger, C.; Mfoumboulou, Y.D. Decentralized Model-Reference Adaptive Control Based Algorithm for Power Systems Inter-Area Oscillation Damping. *Energies* **2022**, *15*, 8762. <https://doi.org/10.3390/en15228762>

Academic Editors:
Abu-Siada Ahmed and Surender Reddy Salkuti

Received: 22 September 2022

Accepted: 18 November 2022

Published: 21 November 2022

Publisher's Note: MDPI stays neutral with regard to jurisdictional claims in published maps and institutional affiliations.



Copyright: © 2022 by the authors. Licensee MDPI, Basel, Switzerland. This article is an open access article distributed under the terms and conditions of the Creative Commons Attribution (CC BY) license (<https://creativecommons.org/licenses/by/4.0/>).

Keywords: MRAC; oscillation damping; inter-area oscillations; Gaussian noise; small-signal stability; SMIB; MATLAB/SIMULINK

1. Introduction

1.1. Background

Power systems are vulnerable to small-signal stability problems as a result of a lack of damping or synchronizing torques [1–3], more notably inadequate damping of oscillations [4]. This vulnerability is due to restricted transmission networks and the present liberalized electrical framework, which pushes power systems closer to their intended technological limits. Power systems are prone to Low-Frequency Electromechanical Oscillations (LFEOs) generated by small fluctuations in the system load. The shift from a stable to an unstable state is undoubtedly induced by a change in the operating condition, resulting in the appearance of contingencies such as ringdown oscillations. A rapid system collapse is therefore expected if not properly damped [5]. As a consequence of the presence of high damping observed in power systems with short lines, oscillations do not cause any problem therein [6]. However, the system's power transfer capability can be highly affected as they represent, under certain operating conditions, a serious threat to the system stability [6,7]. The stability of the rotor angle must be assured when it oscillates due to LFEOs, and hence the ability of the interconnected synchronous machines to maintain synchronism is crucial. The nature of a power system's response to small disturbances is heavily dependent on factors including the initial operating state, the strength of the transmission system, and the type of generator excitation control employed. In the case of generators connected radially to a large power system, the instability is caused by a lack of sufficient synchronization torque in the absence of automated voltage regulators. This issue changes into one of guaranteeing adequate oscillation damping when there are enough acting voltage regulators. Additionally, oscillations of increasing amplitude are typically

indicative of instability [4]. These small disturbances are classified by their interaction characteristics as [6,8]:

- Inter-area mode oscillations;
- Local plant mode oscillations;
- Interplant mode oscillations;
- Torsional (sub-synchronous) mode oscillations;
- Control-mode oscillations.

Alternatively, they can be classified by the operating conditions of the power system as:

- Ambient (spontaneous) oscillations;
- Transient oscillations;
- Forced oscillations.

Inter-area oscillations have been the cause of major blackouts throughout the world [9], with numerous ways to mitigating their impact having been explored since the 1960s. A reasonably complete description of numerous blackouts across the world, including the biggest three, namely, the 14 August 2003 US and Canada blackout, the 28 September 2003 Italian blackout, and the 4 November 2006 European Incident, is presented in [9]. From a study of these events, the voltage collapse, cascade overload, frequency collapse, loss of synchronism, and system separation were listed as causes, with the first two being the major types of incidents leading to such contingencies [7]. Power system oscillations were identified as both initiating and triggering events in all of these accidents. Consequently, there is a need for a control strategy that can implement the necessary corrective action within a short period of time after they occur [7]. The Wide-Area Measurement System (WAMS), which is based on Phasor Measurement Units (PMUs) and the Global Positioning System (GPS), was adopted as a result of the shortcomings of the previously employed SCADA/EMS systems with their 1–5 s measurement intervals, which are unsuitable for any real-time control. WAMS allows system operators to obtain more efficient and speedy real-time system information and achieve real-time control [9]. The oscillations that cause system collapse involve groups of generators in one location swinging against another group in another location. They are referred to as inter-area oscillations. Those involving generators within an area, also known as local oscillations, are generally damped accurately by the standard Power System Stabilizers (PSSs) using generators' speed or speed deviation as inputs. Those stabilizers' outputs feed the excitation system.

Efforts to mitigate such contingencies have led to various control mechanisms being proposed. While the use of decentralized schemes with controllers added at each generating unit was proposed in some of those methods, others opted for centralized architectures where a controller is usually added at the tie-line. However, the authors of [10–12] used methods that can be classified as hybrids in a sense that their proposed controllers comprised a small bit of each of the aforementioned architectures. Oscillation damping controllers considered as having centralized architecture are often referred to as Wide-Area Controllers. Such a controller was proposed by [13] in the form of an optimal control scheme considering nonlinear dynamics associated with the DC-link capacitor voltage. A Wide Area Damping Controller (WADC) based on the Network Predictive Control (NPC) was introduced by [14]. This work extended the authors' previously proposed Generalized Predictive Control (GPC) by taking into consideration and mitigating the impact of communication delays of the wide-area signals from the Wide-Area Measurement System (WAMS). A non-smooth optimization method was introduced by [15] in designing a fixed-order Ricatti-based controller that is said to overcome the limitations of controllers based on H_∞ , as proposed by [16] H_∞ -based control algorithms that have also been employed in decentralized oscillation damping architectures, as described in [17,18]. Other decentralized controllers include [19,20]. While the first group proposed an adaptive fuzzy sliding-mode control through a Wavelet Neural Network (WNN) sliding-mode control, the latter presented an Adaptive Model Predictive Controller (AMPC).

The application of adaptive control in power systems was first documented in the 1980s by [21], who conducted a comparison study between adaptive-based stabilizers and those based on fixed gains and their impact on generator excitation control. The authors chose not to employ algorithms with implicit identification, such as the MRAC, and instead proposed clearly identifiable controllers such as the Optimal Linear Quadratic (LQ) and Pole Assigned (PA) controllers while the adaptive controller is set as a transient gain stabilizer. To enhance the dynamic stability of power systems, the authors in [22] proposed a decentralized multivariable self-tuning adaptive control. A single-input/multiple-output (SIMO) design was instead explored, with the excitation signal as the input and the terminal voltage, shaft speed, and output power as the outputs. This contrasted with many prior designs such as [21], where controllers were applied to the excitation based on a SISO configuration. The authors of [21,22] both argued against the MRAC owing to the difficulties in selecting an adequate reference model. However, as stated in [9], the third and fourth-order representations of synchronous generators are sufficient for controller design. The authors' legitimate concern is therefore narrowed to selecting an appropriate third or fourth-order reference model. Another interesting adaptive control strategy is presented in [23]. Referred to as "Gain-Scheduled Sliding-Mode-Type Iterative Learning Control", it is a combination of Sliding-Mode (SM) control and Iterative Learning (IL) control, which is a memory-based control approach aimed at systems that perform repeated or periodic operations over a finite time domain [23]. MRAC occurrences in power system stability can be found in [24], where it is employed for the design of an adaptive scheme for a Permanent-Magnet (PM) Synchronous Motor, in [25] to improve the Low-Voltage Ride Through (LVRT) capabilities for grid integration of wind energy systems, in [26] to improve transient stability of Virtual Synchronous Generators (VSG), or in [27] to regulate the inner grid and the outside photovoltaic (PV) voltage control loop.

1.2. Contribution of this Manuscript

With power systems being highly nonlinear and prone to disturbances that are often inherent to them, such as small variations in the system load, this paper extends the knowledge in the existing literature by proposing a novel MRAC-based decentralized algorithm. Though the results of the controller presented by [23] are promising, it may not be robust enough to handle the non-stationary type of signals since the main type of disturbances considered are LFEOs which are inherent to power system networks. The proposed controller enhances the rotor angle stability and is thus suitable to mitigate the effect of inter-area oscillations in power systems. Unlike the approaches presented in the literature where controllers are designed based on a linearized model [28,29], the proposed control algorithm is constructed from the nonlinear equations that describe the dynamics of the synchronous generator. Furthermore, the reference model of a MRAC is a shaping filter aimed at achieving a desired command following and can be chosen as a Linear Time-Invariant (LTI) model that captures all of the performance specifications including robustness [30]. A Linear Quadratic Regulator that provides optimally control gains is therefore proposed to stabilize this model.

The novelties of this paper include:

- The application of adaptive control theory in the design of the proposed power system inter-area oscillation damping controller.
- The application of an adaptive augmentation design approach for the controller design, i.e., the nominal controller is augmented with an adaptive controller. This method is more prevalent and more robust than a fully adaptive control design [30].
- The application of Linear Quadratic Regulator (LQR) control theory in the design of the nominal controller. This regulator is aimed at stabilizing the time-invariant reference model.
- The introduction of Gaussian noise as a disturbance to better emulate small variations in the system load and to assess the performance of the proposed control scheme.

1.3. Organisation of the Manuscript

The rest of the paper is organized as follows: Section 2 introduces the synchronous generator dynamics and modelling, with the focus on fourth-order representation. Section 3 presents the proposed MRAC-based oscillation damping controller. The simulation results based on the proposed MRAC-based power system inter-area oscillation damping controller are presented in Section 4. Section 5 covers the discussion of the results, while Recommendations for future works and improvements are proposed in Section 6.

2. Synchronous Generator Dynamics and Modelling

The equation governing the motion of synchronous machines is based on this principle of dynamics:

$$T = \iota \times \alpha \quad (1)$$

where T is the accelerating torque, ι is the moment of inertia, and α is the angular acceleration.

From (1), the following expression can be derived:

$$\frac{2H}{w_{sn}} \frac{d^2 \delta_m}{dt^2} = P_m(pu) - P_e(pu) \quad (2)$$

where H is the ratio between the stored kinetic energy (in megajoules) at the synchronous speed (w_{sn}) over the machine ratio in MVA, δ_m is the angular displacement from the synchronously rotating reference axis, P_m is the mechanical power, and P_e is the electrical power. However, with the system inertia being the intrinsic capacity of online synchronous machines to resist rapid changes in generation or load, the rising participation of renewable generators such as wind and solar to power system networks is mentioned to lead to a decrease in total system inertia [31]. This is resultant from the inability of these renewable energy sources (RES) to provide sufficient inertia to the grid they are connected to [31–33].

In this paper, no RES penetration is considered.

Equation (2) is also referred to as the swing equation, and an inspection of the swing curves of all machines in the system indicates whether they remain in synchronism after a disturbance. Electromechanical oscillations are inherent to all power systems. Hence, the analysis developed has the fundamental aim of understanding these phenomena in qualitative terms. Consequently, reference can be made to the simplest scheme of a generator (or area) connected to an infinite system; this scheme is valid in the case of both local and inter-area oscillations [11]. It is also referred to as a Single Machine Infinite Bus (SMIB). It is this very representation that is used to derive various orders of the synchronous generator, with the word order referring to the set of differential equations used to characterize SMIB. Higher orders such as the third, fourth, fifth, and seventh can also be used to describe it, and details on these equations and the domains where each is applied are found in [4,9,34]. The third-order model is said to be suitable for studying control systems of generators and their synthesis, as well as the dynamic analysis of small-signal stability [9]. As for the fourth-order model, it is sufficiently accurate to analyse electromechanical dynamics [35]. As emphasized by [9], it is suitable to model the generator in the full range of (local and inter-area) electromechanical oscillations. Hence, fourth-order models will be utilized in the controller's design.

2.1. Fourth-Order Model Representation of Synchronous Generators

As illustrated in [11,34,36], the fourth-order model representation of the synchronous generator can be seen as an extension of the third-order model, with the damper winding in the q -axis taken into consideration. This can be written as [11]:

$$\dot{x}_1 = \omega_0 x_2 \quad (3a)$$

$$\dot{x}_2 = \frac{1}{J} (T_m - T_e - D x_2) \quad (3b)$$

$$\dot{x}_3 = \frac{1}{T'_{q0}} \left(-x_4 + (x_q - x'_q) i_q \right) \tag{3c}$$

$$\dot{x}_4 = \frac{1}{T'_{d0}} \left(E_{fd} - x_3 - (x_d - x'_d) i_d \right) \tag{3d}$$

where

$$i_d = \frac{e'_q - V \cos \delta}{x'_q}$$

$$i_q = \frac{V \sin \delta - e'_d}{x'_q}$$

$$P_e \cong \frac{V}{x'_d} e'_q \sin \delta - \frac{V}{x'_q} e'_d \cos \delta + \frac{V^2}{2} \left(\frac{1}{x'_q} - \frac{1}{x'_d} \right) \sin(2\delta)$$

T'_{q0} : q-axis open-circuit time constant

e'_q : q-axis transient emf

e'_d : d-axis transient emf

Let

$$\underline{\mathbf{X}} = \begin{bmatrix} x_1 \\ x_2 \\ x_3 \\ x_4 \end{bmatrix} = \begin{bmatrix} \delta \\ \omega \\ e'_d \\ e'_q \end{bmatrix} \text{ and } \underline{\mathbf{U}} = \begin{bmatrix} u_1 \\ u_2 \end{bmatrix} = \begin{bmatrix} E_{FD} \\ P_m \end{bmatrix} \tag{4a}$$

The state-space representation can be written as in Equation (4b):

$$\dot{\mathbf{X}} = \begin{bmatrix} 0 & 1 & 0 & 0 \\ 0 & -\frac{D}{J} & 0 & 0 \\ 0 & 0 & -\frac{1}{x'_q T'_{q0}} (x'_q + x_q - x'_d) & 0 \\ 0 & 0 & 0 & -\frac{1}{T'_{d0}} \left(\frac{x'_d}{x'_d} \right) \end{bmatrix} \begin{bmatrix} \delta \\ \omega \\ e'_d \\ e'_q \end{bmatrix} + \begin{bmatrix} 0 & 0 \\ 0 & -\frac{1}{J} \\ 0 & 0 \\ \frac{1}{T'_{d0}} \end{bmatrix} \begin{bmatrix} E_{FD} \\ P_m \end{bmatrix} + \begin{bmatrix} 0 \\ \frac{1}{J} \left(\frac{e'_d V}{x'_q} \cos \delta - \frac{e'_q V}{x'_d} \sin \delta - \frac{V^2}{2} \sin 2\delta \left(\frac{1}{x'_q} - \frac{1}{x'_d} \right) \right) \\ \frac{V}{T'_{q0}} \left(\frac{x_q - x'_d}{x'_q} \right) \sin \delta \\ \frac{V}{T'_{d0}} \left(\frac{x'_d}{x'_d} - 1 \right) \cos \delta \end{bmatrix} \tag{4b}$$

2.2. Synchronous Generator Modelling

Ambient inter-area oscillations occur in power systems due to poor damping and are mainly excited by constantly varying loads. “Inter-area oscillation is a complex and nonlinear phenomenon, and its damping characteristic is dictated by the strength of the transmission path, the nature of loads, the power flow through interconnections and the interaction of the loads with the dynamics of generators and their associated controls” [6,37,38].

While ordinarily stable, with enough stress, oscillations may cause the Hopf bifurcation to occur where the real parts of the complex conjugate eigenvalue pair cross the imaginary axis making the system unstable [6,39]. Because of the high impedance, the generator’s amortisseur windings lose their effect on inter-area oscillation damping. The same is true for adverse interactions between automated controls, particularly Automatic Voltage Regulators (AVRs) [7]. Regardless of the potential adverse effects of the automated controls, when the transmission path is weak, the uncontrolled system damping for these type of oscillations is frequently low [9]. Additionally, when the interconnecting lines’ loading increases, the damping decreases. This is due to the increasing angle difference between oscillating generator groups, with the voltage oscillations at each generator terminal causing the AVRs to act, resulting in negative damping [6,9]. To mitigate the effect of such oscillations, knowledge of the system characteristics is of the utmost importance. The system characteristics through its rotor angle are presented in Figure 1 with the focus being on the fourth-order representation model since it encompasses the third. Furthermore, this representation will be the only one utilized for the remainder of this paper.

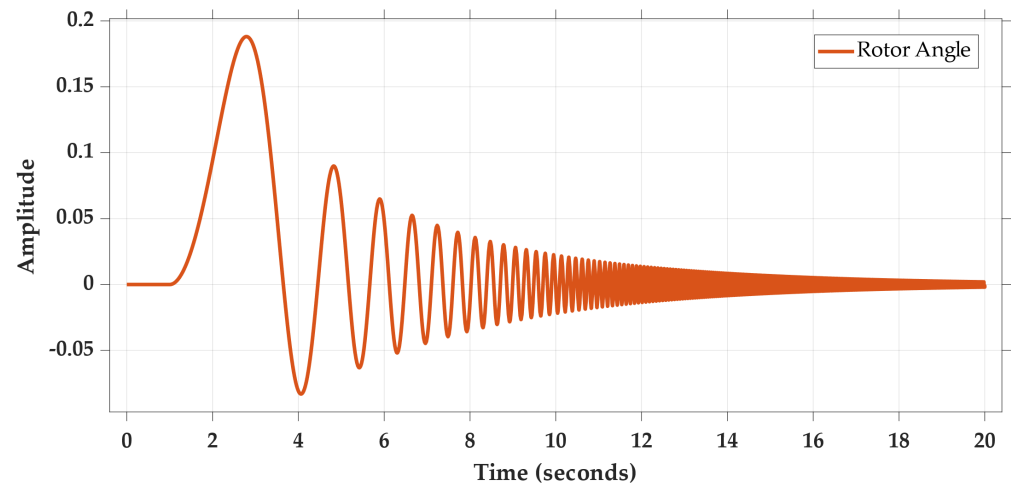


Figure 1. Synchronous generator rotor angle when $E_{FD} = 1$, $P_m = 1$, and no initial conditions.

3. Proposed Model-Reference Adaptive Control for Power System Inter-Area Oscillation Damping

3.1. Background

Designing a controller for a given system implies learning how that very system behaves physically, and this is oftentimes achieved through its mathematical representation [30]. As shown in Equation (6), the synchronous generator dynamics possess parameter variations that are due to their very nonlinear structure. Hence, reducing the system uncertainty as much as practically possible is of the utmost importance. This section is structured as follows. Firstly, an overview of the composition of such a controller is introduced. Thereafter, the structure of the MRAC for the synchronous generator is presented. Two classes of adaptive control schemes are generally identified: the direct and indirect methods [30,40,41]. Though either one of the classes are used in adaptive control architectures, often, they are combined and referred to as composite [30,41], combined, or hybrid-direct adaptive control [30,42]. Further reading in relation to the MRAC can be found in [30,40,43], with Figure 2 showing the structure of the MRAC system. The proposed controller uses the direct method.

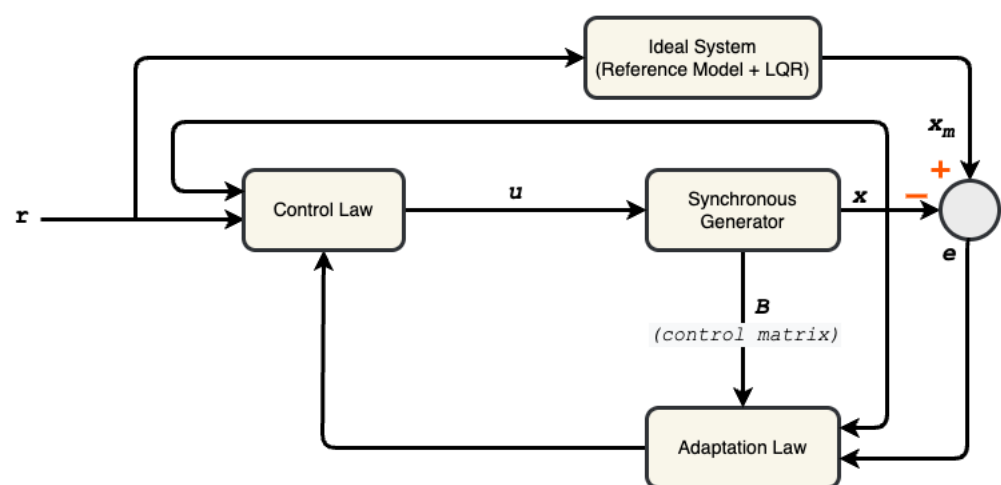


Figure 2. Typical Model-Reference Adaptive Control structure.

The adaptive control is formulated as a tracking control problem where the adaptation is aimed at tracking the error between a given reference model and the system output [30]. In a sense, the former is a shaping filter that is used to achieve the desired behaviour. This

error can either be based on system states or output error. From the above, it is therefore important that it is well designed. Considering that the objective of an adaptive control system is to adapt to a given system's uncertainty so that the tracking error is minimized ($e(t) \rightarrow 0$), the states of this very system must follow the reference model perfectly, i.e., $x(t) \rightarrow x_m(t)$ [30].

3.2. Controller Design

Figure 3 depicts the steps followed in the design of the proposed controller. An LQR controller is applied to the model matching reference model. The error dynamics are then used in the adaptation law which, combined with the nominal controller (LQR), constitute the control signal.

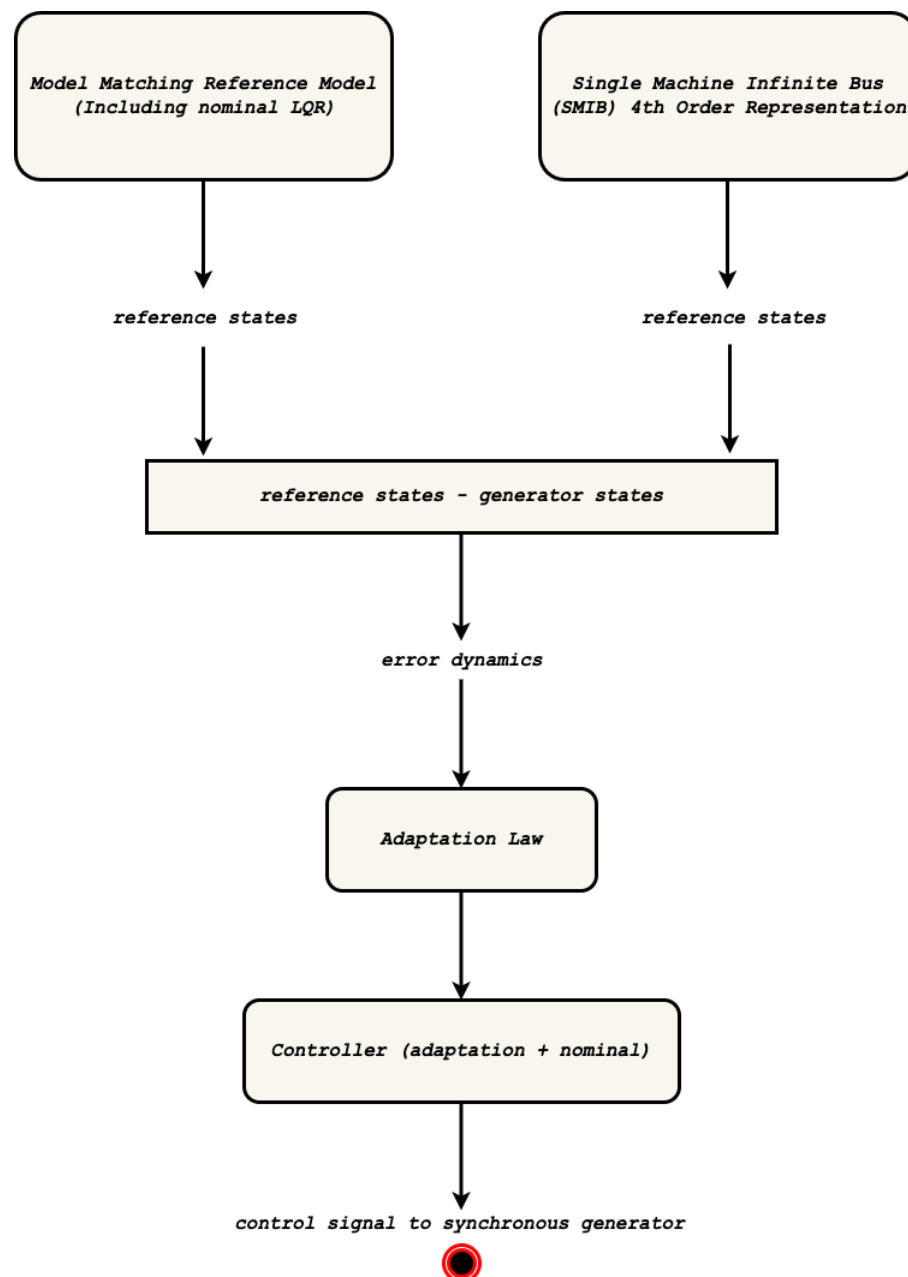


Figure 3. MRAC design architecture for power system inter-area oscillation damping structure.

Equation (6) can be rewritten as $\dot{x} = AX + BU + f(x)$. This can be further modified as in Equation (5):

$$\dot{x} = f(x) + B \left[u + B^T (BB^T)^{-1} \Theta^{*T} \Phi(x) \right] \quad (5)$$

where $B \in \mathbb{R}^n \times \mathbb{R}^m$ is a full-rank, non-square wide matrix with $n < m$ and $\text{rank}(B) = n$ [30], $\Theta^* \in \mathbb{R}^l \times \mathbb{R}^m$ is a constant, unknown matrix, and $\Phi(x) \in \mathbb{R}^l$ is a vector of known and bounded basis functions. $B^T (BB^T)^{-1}$ is the right pseudo-inverse of the control matrix and $(BB^T)^{-1}$ must exist to avoid singularity in the controller.

\exists (Adjustable control gains) K_x and K_r that satisfy the model matching conditions as described in Equation (6a,b) [30]:

$$A + BK_x = A_m \quad (6a)$$

$$BK_r = B_m \quad (6b)$$

LQR control theory is employed to find the optimal feedback matrix that will ensure the stability of the chosen reference model. The derivations are shown in Appendix A. Considering Equation (5), the adaptive controller is therefore designed as:

$$u = u_n + u_a \quad (7)$$

where

$u_n = K_x x + K_r r$ is the nominal controller.

$u_a = -B^T (BB^T)^{-1} \Theta^T \Phi(x)$ is the adaptation component.

Defining $\tilde{\Theta}(t) = \Theta(t) - \Theta^*$ as the estimation error, the closed-loop synchronous generator model is expressed as:

$$\dot{x} = (A + BK_x)x + BK_r r - B^T (BB^T)^{-1} \tilde{\Theta}^T \Phi(x) \quad (8)$$

Thus, the closed-loop tracking error is described as:

$$\dot{e} = \dot{x}_m - \dot{x} = A_m e + B^T (BB^T)^{-1} \tilde{\Theta}^T \Phi(x) \quad (9)$$

Choosing the following Lyapunov candidate [30]

$$\dot{V} = -\Gamma \Phi(x) e^T P B \quad (10)$$

and from Barbalat's lemma, the tracking error can be shown to be asymptotically stable with $e(t) \rightarrow 0, \forall t \rightarrow \infty$ [30].

4. Simulation Results

The results are presented in the form of case studies starting from the steady state condition. The performance of the proposed algorithm is assessed by setpoints change, disturbances in the input signal, and faults at $t = 3$ s and $t = 9$ s, as well as the introduction of internal disturbances. These are assumed to have the characteristics of Gaussian noise with a variance of unity and a sample time of 0.001. Furthermore, they are aimed at replicating low-frequency inter-area oscillations caused by small variations in loads. The simulations are conducted with no initial conditions, and the initial set-points are $E_{FD} = 1$ and $P_m = 1$. Figures 4–9 show the system response for each of the case studies. With angle instability being the root cause of inter-area oscillations, the system's response in this section will refer to the rotor angle's response. A detailed summary of parameters used in the simulations can be found in Appendix B.

Case Study 1. *Steady state with no initial conditions.*

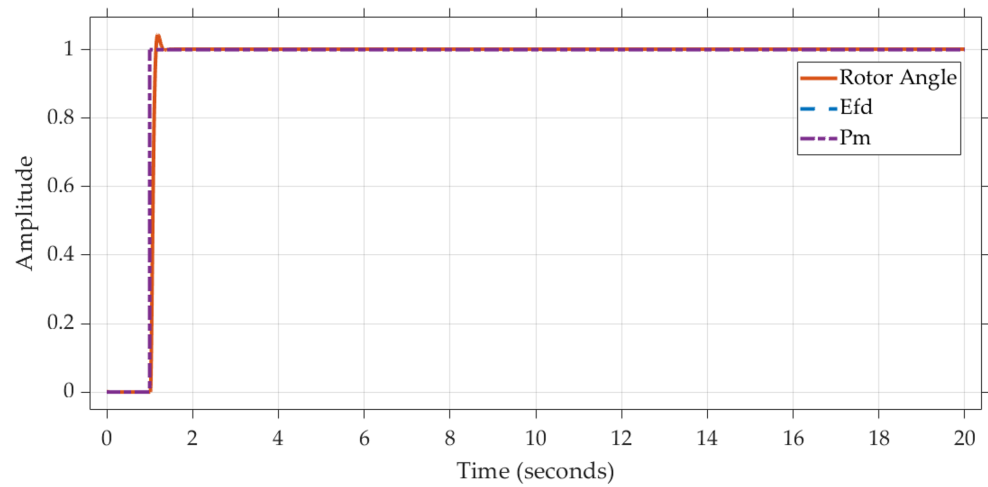


Figure 4. Rotor angle when $E_{FD} = 1$, $P_m = 1$, and learning rate = 10.

Case Study 2. Setpoints change— $E_{FD} = 2.395$ with no initial conditions.

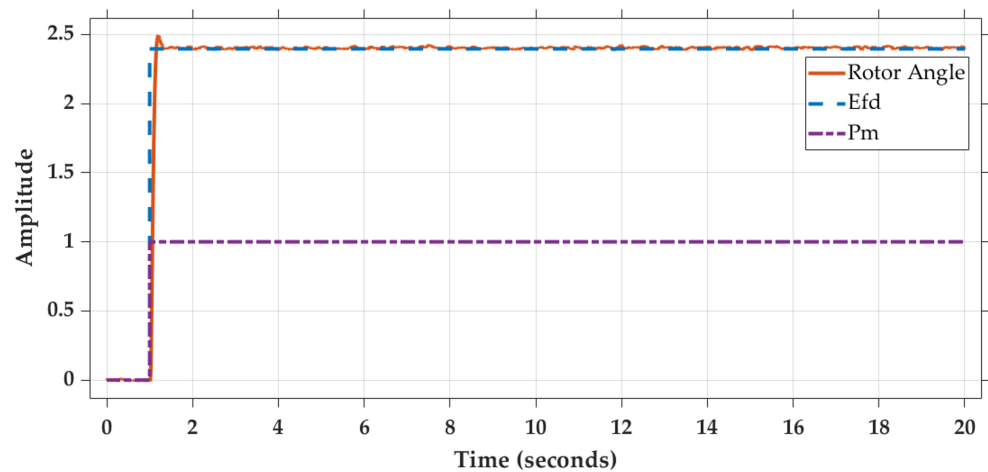


Figure 5. Rotor angle when $E_{FD} = 2.395$, $P_m = 1$, and learning rate = 10.

Case Study 3. Setpoints change— $P_m = 0.77778$ and no initial conditions.

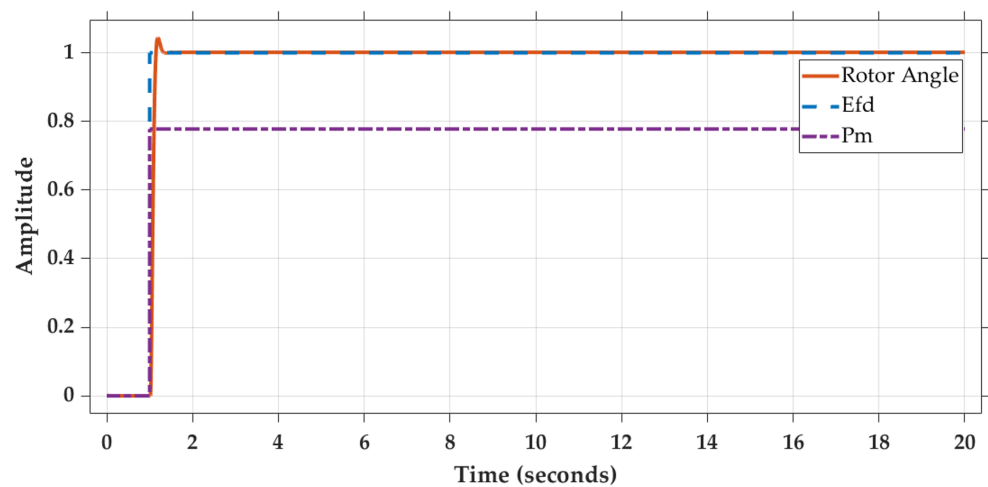


Figure 6. Rotor angle when $E_{FD} = 1$, $P_m = 0.77778$, and learning rate = 10.

Case Study 4. Added disturbances at $t = 0$ s and no initial conditions.

A normally (Gaussian) distributed random signal with a variance of 1 and 0.001 sample time is added onto the system. In all subsequent test cases, and whenever internal or external noise is added onto the system, the signal with the characteristics illustrated in Figure 7a is utilized. Furthermore, to better emulate inter-area oscillations which are inherent to a given power system, this noise is added at the very beginning of the simulation. While external disturbances in this paper pertain to noise added onto the input signal, internal disturbances pertain to those that make the very system.

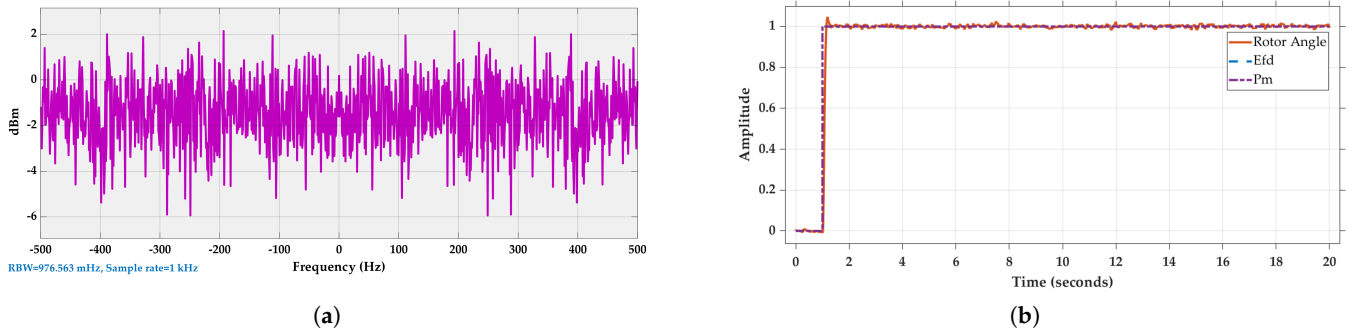


Figure 7. Synchronous generator subjected to Gaussian noise. (a) Gaussian noise characteristics; (b) rotor angle when $E_{FD} = 1$, $P_m = 1$, and learning rate = 10.

Case Study 5. Added fault at $t = 9$ s for a duration of ~ 300 ms—No setpoint change and no initial conditions.

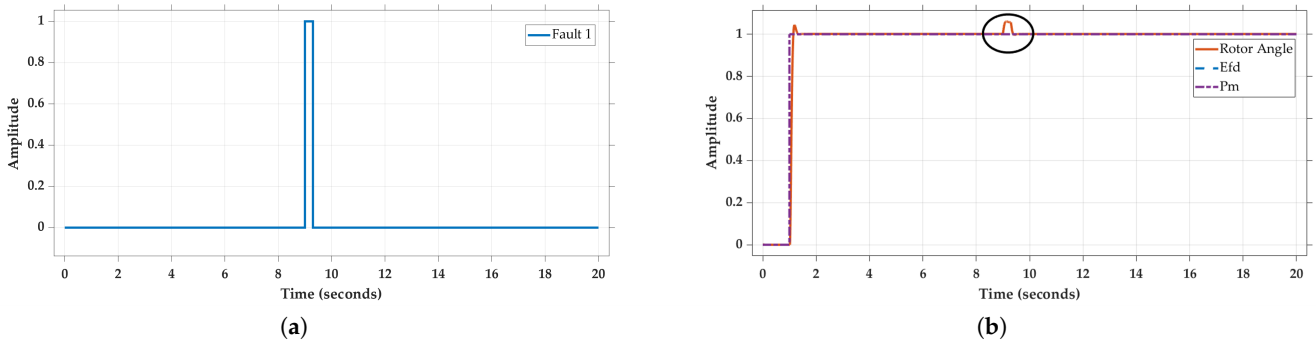


Figure 8. Synchronous generator subjected to fault at $t = 9$ s. (a) Fault characteristics; (b) rotor angle when $E_{FD} = 1$, $P_m = 1$, learning rate = 10, and fault at $t = 9$ s.

Case Study 6. Two added faults at $t = 3$ s and $t = 9$ s for a duration of ~ 100 ms and ~ 300 ms, respectively. Furthermore, setpoints have been changed and disturbances in the form of Gaussian noise, whose characteristics are presented in Figure 8a, are added.

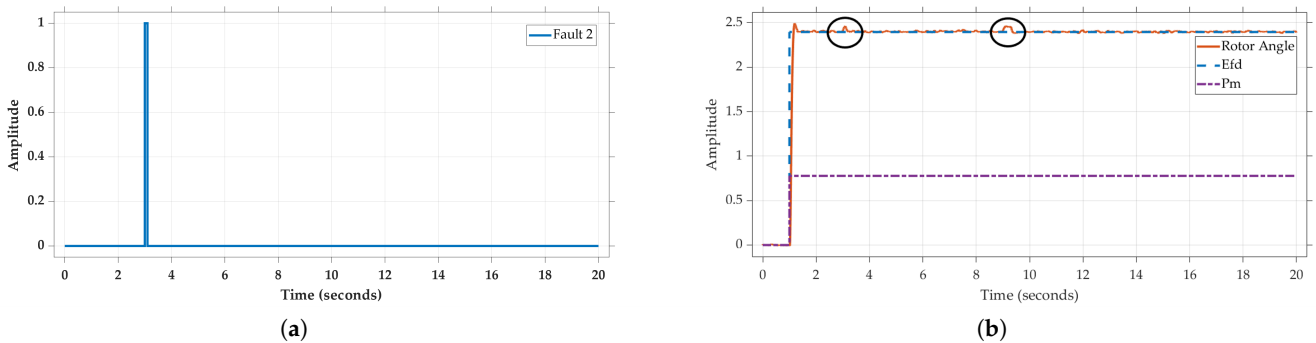


Figure 9. Synchronous generator subjected to Gaussian noise and fault at $t = 3$ s and $t = 9$ s, respectively. (a) $t = 3$ s fault characteristics; (b) rotor angle when $E_{FD} = 1$, $P_m = 1$, learning rate = 10, and faults.

5. Discussion

To validate the proposed MRAC-based oscillation damping controller, the synchronous generator was subjected to various contingencies. They varied from setpoint changes in its two inputs, namely E_{FD} and P_m , to faults. Furthermore, to emulate small variations in loads that are mainly responsible for inter-area oscillations, internal disturbances were added. Notwithstanding the type of disturbances, the rotor angle maintained a considerably stable response, with an overshoot of less than 5%, a rise time less than 100 ms, non-existent steady-state error, and a good recovery time of less than 800 ms. This recovery time was achieved when the generator was subjected to disturbances in the form of a normally (Gaussian) distributed random signal with a variance of 1 and 0.001 sample time, setpoint changes, as well as faults. The latter were introduced at the third and ninth second for a duration of 100 ms and 300 ms, respectively. The synchronous generator, through its rotor angle, remained stable irrespective of the contingencies. Furthermore, considering the time of interest is 3–5 s for standard power systems and 10 s for large ones with weak interconnections, the proposed novel scheme is very robust. The various test cases together with their results are summarized in Table 1. Characteristics such as the rotor angle's rise time, overshoot, and recovery time are presented therein. Nevertheless, this can be further refined by taking into consideration the penetration of RES into power system grids as they affect the overall system inertia.

Table 1. Simulation results of the proposed MRAC.

	E_{FD}	P_m	Gaussian Noise	Fault	Rise Time (ms)	Slew Rate (/s)	Overshoot (%)	Steady-State Error (%)	Recovery Time (ms)
Case 1	1	1	0	0	83.308	21.528	4.737	N/A	N/A
Case 2	2.395	1	0	0	88.852	21.528	3.646	N/A	N/A
Case 3	1	0.77778	0	0	83.314	9.525	4.737	N/A	N/A
Case 4	1	1	Internal	0	86.433	9.301	4.737	N/A	N/A
Case 5	1	1	0	Impulse t = 9 s	84.207	9.475	4.147	N/A	N/A
Case 6	2.395	0.77778	Internal and to input signal	Impulse t = 3 s and t = 9 s	87.784	9.218	4.046	N/A	~350 & ~720

Another aspect to consider is saturation. From the simulations, the inputs are bounded such that $E_{FD}, P_m \in [0.1, 4]$ without disturbance and $E_{FD}, P_m \in [0.7, 4]$ when disturbances are introduced. This shown in Figure 10a–c.

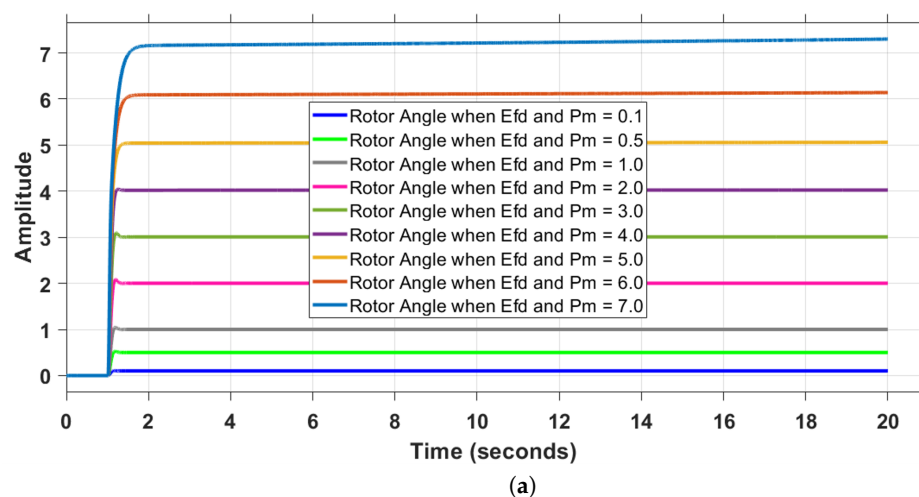


Figure 10. Cont.

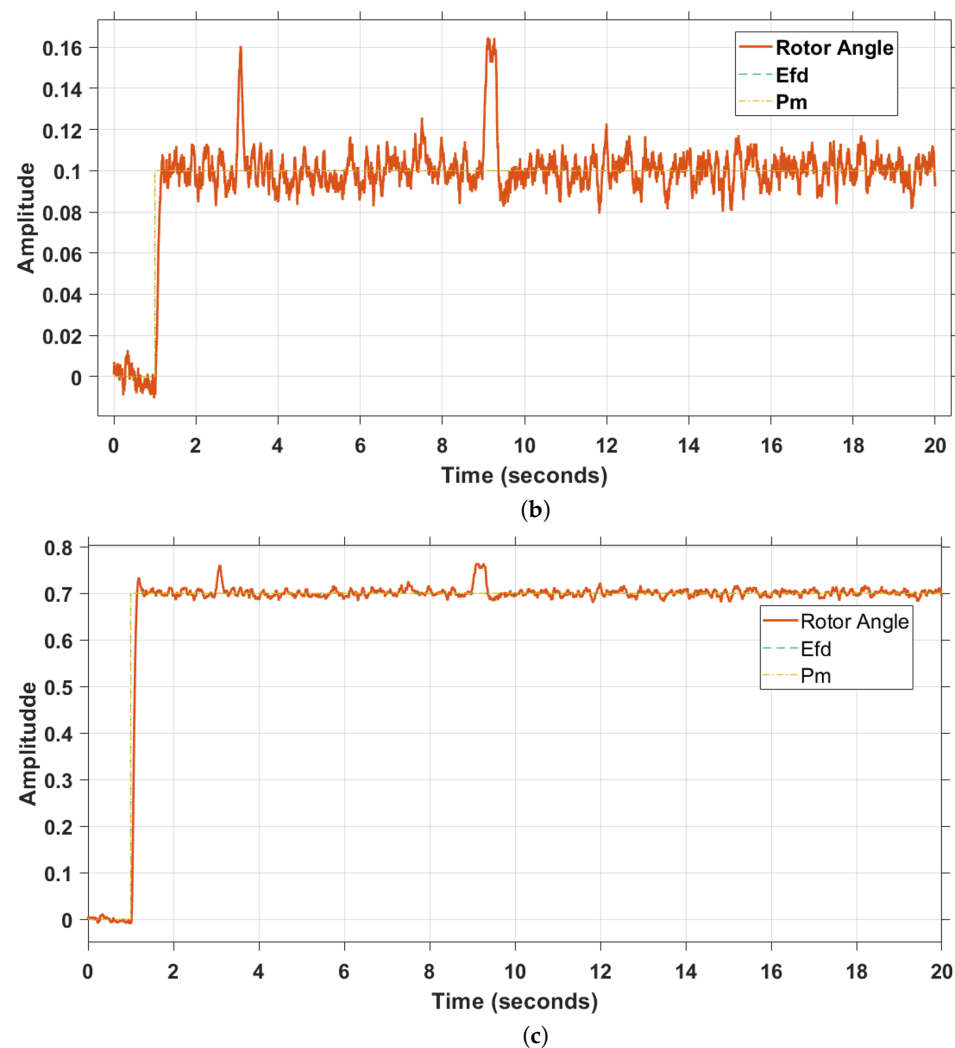


Figure 10. Synchronous generator rotor angle with bounded inputs. (a) Inputs varied from 0.1 to 7 without disturbance; (b) inputs at 0.1 with Gaussian noise; (c) inputs at 0.7 with noise.

Therefore, the performance of the proposed controller cannot be guaranteed for input values $\in [5, \infty]$ without disturbance and for values $\in ([-\infty, 0.7] \cup [4, +\infty])$ when subjected to disturbances. Moreover, the adaptation gain is limited to values $\in [2, 100]$.

6. Recommendations

The control algorithm presented in this paper can be further refined so that robustness is ensured with a fast adaptation. This can be achieved by utilising \mathcal{L}_1 adaptive control theory. With this type of architecture, the adaptation is decoupled from robustness, and the transient performance together with the said robustness are guaranteed in the presence of fast adaptation [44]. As for its validation, an IEC-61850-based hardware-in-the-loop setup in lieu of a simulation-based approach can be explored for real-time implementation. A real-time hardware platform such as the Real-Time Digital Simulator would be ideal for real-time implementation. Taking into consideration RES penetration, this work can be further refined by leveraging the work of [31–33] to ensure that the inertia of the system is maintained. Lastly, the controller presented in [23] can be explored for transient stability and perhaps modified for small-signal rotor angle stability enhancement.

Author Contributions: Conceptualization, T.-w.P.-P.B.-B., Y.D.M., and C.K.; methodology, T.-w.P.-P.B.-B.; software, T.-w.P.-P.B.-B.; validation, T.-w.P.-P.B.-B.; formal analysis, T.-w.P.-P.B.-B.; investigation, T.-w.P.-P.B.-B.; resources, T.-w.P.-P.B.-B., Y.D.M., and C.K.; data curation, T.-w.P.-P.B.-B.; writing—

original draft preparation, T.-w.P.-P.B.-B.; writing—review and editing, T.-w.P.-P.B.-B.; visualization, T.-w.P.-P.B.-B.; supervision, Y.D.M. and C.K. All authors have read and agreed to the published version of the manuscript.

Funding: This research received no external funding.

Data Availability Statement: Not applicable.

Conflicts of Interest: The authors declare no conflict of interest.

Appendix A. Linear Quadratic Regulator

Given $\dot{x}_m = A_m x_m + B_m u_m$, the quadratic optimal regulator problem implies finding the matrix K of the optimal control vector $u_m(t) = -Kx_m(t)$ to minimize the performance index. This optimal configuration is illustrated in Figure A1.

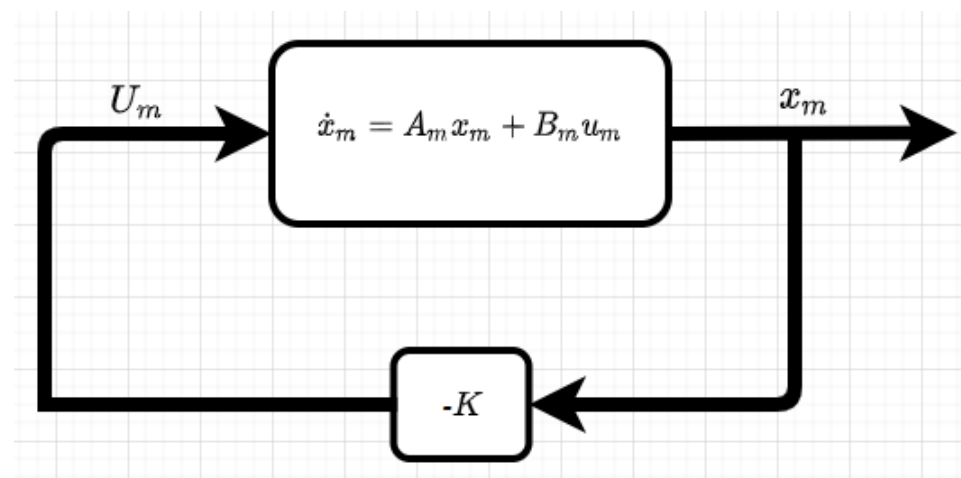


Figure A1. Optimal regulator.

From Figure A1, \dot{x}_m is the reference model's dynamics, with the performance index expressed as [35]:

$$J = \int_0^{\infty} (x_m^T Q x_m + u_m^T R u_m) dt \quad (\text{A1})$$

where

Q : can be either a positive-definite Hermitian, a positive semi-definite Hermitian, or a real symmetric matrix.

R : positive-definite Hermitian or real symmetric matrix.

The optimal matrix K of the optimal control vector can be expressed as [36]:

$$K = (T^T)^{-1} B_m^T P = R^{-1} B_m^T P \quad (\text{A2})$$

with $R = T^T T$.

Let P be a positive-definite Hermitian or real symmetric matrix, then the optimal control law $u_m(t) = -Kx_m(t)$ can thus be given by:

$$u_m(t) = -R^{-1} B_m^T P x_m(t) \quad (\text{A3})$$

with the expression of P derived from the *reduced-matrix Riccati equation* below [36]:

$$A_m^T P + P A_m - P B_m R^{-1} B_m^T P + Q = 0 \quad (\text{A4})$$

Appendix B. Generator Parameters

Table A1. Synchronous generator parameters [9].

Acronym	Value
x_d	1.8 p.u
x'_d	0.3 p.u
x_q	1.7 p.u
x'_q	0.55 p.u
x''_q	0.25 p.u
x''_d	0.25 p.u
D	0
H	6.5
S	900 MVA
T'_{q0}	0.4 s
T'_{d0}	8 s
T''_{d0}	0.03 s
T''_{q0}	0.05 s

References

- Vittal, V. Consequence and Impact of Electric Utility Industry Restructuring on Transient Stability and Small-Signal Stability Analysis. *Proc. IEEE* **2000**, *88*, 196–207. [\[CrossRef\]](#)
- Morison, K.; Wang, L.; Kundur, P. Power System Security Assessment. *IEEE Power Energy Mag.* **2004**, *2*, 30–39. [\[CrossRef\]](#)
- Rueda, J.L.; Juárez, C.A.; Erlich, I. Wavelet-Based Analysis of Power System Low-Frequency Electromechanical Oscillations. *IEEE Trans. Power Syst.* **2011**, *26*, 1733–1743. [\[CrossRef\]](#)
- Kundur, P. *Power System Stability and Control*; McGraw-Hill Education: New York, NY, USA, 1994; p. 1176.
- Rogers, G. *Power System Oscillations*; Springer Science & Business Media: Berlin/Heidelberg, Germany, 2000.
- Turunen, J. A Wavelet-Based Method for Estimating Damping in Power Systems. Ph.D. Thesis, Aalto University, Espoo, Finland, 2011.
- Banga-Banga, T.-W.P.-P. Model-Reference Adaptive Control Algorithm for Power System Interarea Oscillations Damping. Master's Thesis, Cape Peninsula University of Technology, Cape Town, South Africa, 2022; p. 272.
- Khairudin, F. Synchrophasor Measurement Based Mode Detection and Damping Estimation in Power System Using Fft-Continuous Wavelet Transform Approach. Ph.D. Thesis, Kyushu Institute of Technology, Fukuoka, Japan, 2016.
- Eremia, M.; Shahidehpour, M. *Handbook of Electrical Power System Dynamics*; John Wiley & Sons: Hoboken, NJ, USA, 2013; ISBN 978-1-118-49717-3.
- Morsali, J.; Kazemzadeh, R.; Azizian, M.R.; Parhizkar, A. Introducing PID-Based PSS2B Stabilizer in Coordination with TCSC Damping Controller to Improve Power System Dynamic Stability. In Proceedings of the 22nd Iranian Conference on Electrical Engineering, ICEE 2014, Tehran, Iran, 20–22 May 2014; pp. 836–841.
- Gholinezhad, J.; Ebadian, M.; Aghaebrahimi, M.R. Coordinated Design of PSS and SSSC Damping Controller Considering Time Delays Using Biogeography-Based Optimization Algorithm. In Proceedings of the 30th Power System Conference, PSC 2015, Tehran, Iran, 23–25 November 2015; pp. 1–7.
- Fan, R.; Wang, S.; Huang, R.; Lian, J.; Huang, Z. Wide-Area Measurement-Based Modal Decoupling for Power System Oscillation Damping. *Electr. Power Syst. Res.* **2020**, *178*, 106022. [\[CrossRef\]](#)
- Juan, L.; Sheng, D.; Xingfu, Z. A Nonlinear Control Approach to Increase Power Oscillations Damping by SSSC. In Proceedings of the 2008 International Conference on Computer and Electrical Engineering, ICCEE 2008, Phuket, Thailand, 20–22 December 2008; pp. 734–738.
- Yao, W.; Jiang, L.; Wu, Q.H.; Wen, J.Y.; Cheng, S.J. Design of Wide-Area Damping Controllers Based on Networked Predictive Control Considering Communication Delays. In Proceedings of the IEEE PES General Meeting, PES 2010, Minneapolis, MN, USA, 25–29 July 2010.
- Maherani, M.; Erlich, I.; Krost, G. Fixed Order Non-Smooth Robust H_∞ Wide Area Damping Controller Considering Load Uncertainties. *Int. J. Electr. Power Energy Syst.* **2020**, *115*, 105423. [\[CrossRef\]](#)
- Patel, A.; Ghosh, S.; Folly, K.A. Inter-Area Oscillation Damping with Non-Synchronized Wide-Area Power System Stabilizer. *IET Gener. Transm. Distrib.* **2018**, *12*, 3070–3078. [\[CrossRef\]](#)
- Hashmani, A.A.; Erlich, I. Mode Selective Damping of Power System Electromechanical Oscillations Considering Time Delay Uncertainty in Supplementary Remote Signals. *IFAC Proc. Vol.* **2011**, *44*, 6104–6109. [\[CrossRef\]](#)
- Maherani, M.; Erlich, I. Robust Decentralized Fixed Order Wide Area Damping Controller. *IFAC-Pap.* **2018**, *51*, 438–443. [\[CrossRef\]](#)
- Farahani, M.; Ganjefar, S. Intelligent Power System Stabilizer Design Using Adaptive Fuzzy Sliding Mode Controller. *Neurocomputing* **2017**, *226*, 135–144. [\[CrossRef\]](#)

20. Khosravi-Charmi, M.; Amraee, T. Wide Area Damping of Electromechanical Low Frequency Oscillations Using Phasor Measurement Data. *Int. J. Electr. Power Energy Syst.* **2018**, *99*, 183–191. [[CrossRef](#)]
21. Ghosh, A.; Ledwich, G.; Malik, O.P.; Hope, G.S. Power System Stabilizer Based on Adaptive Control Techniques. *IEEE Trans. Power Appar. Syst.* **1983**, *PAS-103*, 1983–1989. [[CrossRef](#)]
22. Fan, J.Y.; Ortmeyer, T.H.; Mukundan, R. Power System Stability Improvement with Multivariable Self-Tuning Control. *IEEE Trans. Power Syst.* **1990**, *5*, 227–234. [[CrossRef](#)]
23. Yao, Q.; Jahanshahi, H.; Bekiros, S.; Mihalache, S.F.; Alotaibi, N.D. Gain-Scheduled Sliding-Mode-Type Iterative Learning Control Design for Mechanical Systems. *Mathematics* **2022**, *10*, 3005. [[CrossRef](#)]
24. Kim, K.H. Model Reference Adaptive Control-Based Adaptive Current Control Scheme of a PM Synchronous Motor with an Improved Servo Performance. *IET Electr. Power Appl.* **2009**, *3*, 8–18. [[CrossRef](#)]
25. Mosaad, M.I. Model Reference Adaptive Control of STATCOM for Grid Integration of Wind Energy Systems. *IET Electr. Power Appl.* **2018**, *12*, 605–613. [[CrossRef](#)]
26. Wu, H.; Wang, X. A Mode-Adaptive Power-Angle Control Method for Transient Stability Enhancement of Virtual Synchronous Generators. *IEEE J. Emerg. Sel. Topics Power Electron.* **2020**, *8*, 1034–1049. [[CrossRef](#)]
27. Bhunia, M.; Subudhi, B.; Ray, P.K. Design and Real-Time Implementation of Cascaded Model Reference Adaptive Controllers for a Three-Phase Grid-Connected PV System. *IEEE J. Photovolt.* **2021**, *11*, 1319–1331. [[CrossRef](#)]
28. Abd El-Kareem, A.H.; Abd Elhameed, M.; Elkholy, M.M. Effective Damping of Local Low Frequency Oscillations in Power Systems Integrated with Bulk PV Generation. *Prot. Control. Mod. Power Syst.* **2021**, *6*, 41. [[CrossRef](#)]
29. Bayu, E.S.; Khan, B.; Ali, Z.M.; Alaas, Z.M.; Mahela, O.P. Mitigation of Low-Frequency Oscillation in Power Systems through Optimal Design of Power System Stabilizer Employing ALO. *Energies* **2022**, *15*, 3809. [[CrossRef](#)]
30. Nguyen, N.T. *Advanced Textbooks in Control and Signal Processing Model-Reference Adaptive Control A Primer*; Springer International Publishing: Berlin/Heidelberg, Germany, 2018; ISBN 978-3-319-56393-0.
31. Carlini, E.M.; Del Pizzo, F.; Giannuzzi, G.M.; Lauria, D.; Mottola, F.; Pisani, C. Online Analysis and Prediction of the Inertia in Power Systems with Renewable Power Generation Based on a Minimum Variance Harmonic Finite Impulse Response Filter. *Int. J. Electr. Power Energy Syst.* **2021**, *131*, 107042. [[CrossRef](#)]
32. Sun, M.; Feng, Y.; Wall, P.; Azizi, S.; Yu, J.; Terzija, V. On-Line Power System Inertia Calculation Using Wide Area Measurements. *Int. J. Electr. Power Energy Syst.* **2019**, *109*, 325–331. [[CrossRef](#)]
33. Akbari, M.; Madani, S.M. A New Method for Contribution of DFIG-Based Wind Farms in Power System Frequency Regulation. In Proceedings of the North American Power Symposium 2010, Arlington, TX, USA, 26–28 September 2010; pp. 1–6.
34. Zacharia, L.; Asprou, M.; Kyriakides, E. Wide Area Control of Governors and Power System Stabilizers with an Adaptive Tuning of Coordination Signals. *IEEE Open Access J. Power Energy* **2019**, *7*, 70–81. [[CrossRef](#)]
35. Machowski, J.; Bialek, J.W.; Bumby, J.R.; James, R. *Power System Dynamics: Stability and Control*; Wiley: Hoboken, NJ, USA, 2008; ISBN 978-1-119-96505-3.
36. Ghahremani, E.; Kamwa, I. Local and Wide-Area PMU-Based Decentralized Dynamic State Estimation in Multi-Machine Power Systems. *IEEE Transactions on Power Syst.* **2016**, *31*, 547–562. [[CrossRef](#)]
37. Pal, B.; Chaudhuri, B. *Robust Control in Power Systems*; Springer Science & Business Media: Berlin/Heidelberg, Germany, 2005. [[CrossRef](#)]
38. Messina, A.R. *Inter-Area Oscillations in Power Systems: A Nonlinear and Nonstationary Perspective*; Messina, A.R., Ed.; Springer: Berlin/Heidelberg, Germany, 2009; ISBN 978-1-4419-4707-9.
39. Mithulananthan, N.; Canizares, C.A.; Reeve, J.; Rogers, G.J. Comparison of PSS, SVC, and STATCOM Controllers for Damping Power System Oscillations. *IEEE Trans. Power Syst.* **2003**, *18*, 786–792. [[CrossRef](#)]
40. Åström, K.J.; Karl, J.; Wittenmark, B. *Adaptive Control*; Addison-Wesley: Boston, MA, USA, 1995; ISBN 978-0-201-55866-1.
41. Lavretsky, E. Combined/Composite Model Reference Adaptive Control. *IEEE Trans. Autom. Control.* **2009**, *54*, 2692–2697. [[CrossRef](#)]
42. Ishihara, A.K.; Al-Ali, K.; Adami, T.; Kulkarni, N.; Nguyen, N. Modeling Error Driven Robot Control. In Proceedings of the AIAA Infotech at Aerospace Conference and Exhibit and AIAA Unmanned...Unlimited Conference, Seattle, DC, USA, 6–9 April 2009; American Institute of Aeronautics and Astronautics Inc.: Reston, VA, USA, 2009.
43. Ioannou, P.; Baldi, S. Robust Adaptive Control. In *The Control Systems Handbook: Control System Advanced Methods*, 2nd ed.; Prentice-Hall, Inc.: Hoboken, NJ, USA, 2010; ISBN 978-1-4200-7365-2.
44. Hovakimyan, N.; Cao, C. *L1 Adaptive Control Theory: Guaranteed Robustness with Fast Adaptation (Advances in Design and Control)*; Society for Industrial and Applied Mathematics: Philadelphia, PA, USA, 2010.